

Influence of polystyrene nanoparticles on the toxicity of tetrabromobisphenol A in human intestinal cell lines

Patricia Soto-Bielicka¹, Ana Peropadre^{*,2}, Soledad Sanz-Alf  rez³, Mar  a Jos   Hazen⁴, Paloma Fern  ndez Freire^{*,5}

Department of Biology, Faculty of Sciences, Universidad Aut  noma de Madrid, Madrid, Spain

ARTICLE INFO

Keywords:

TBBPA
Polystyrene nanoparticles
Cytotoxicity
Human intestinal cell lines
Genotoxicity
Oxidative stress

ABSTRACT

Research and regulatory efforts in toxicology are increasingly focused on the development of suitable non-animal methodologies for human health risk assessment. In this work we used human intestinal Caco-2 and HT29/MTX cell lines to address the potential risks of mixtures of the emerging contaminants tetrabromobisphenol A (TBBPA) and commercial polystyrene nanoparticles (PSNPs). We employed different *in vitro* settings to evaluate basal cytotoxicity through three complementary endpoints (metabolic activity, plasmatic, and lysosomal membrane integrity) and the induction of the oxidative stress and DNA damage responses with specific endpoints. Although no clear pattern was observed, our findings highlight the predominant impact of TBBPA in the combined exposures under subcytotoxic conditions and a differential behavior of the Caco-2 and HT29/MTX co-culture system. Distinctive outcomes detected with the mixture treatments include reactive oxygen species (ROS) increases, disturbances of mitochondrial inner membrane potential, generation of alkali-sensitive sites in DNA, as well as significant changes in the expression levels of relevant DNA and oxidative stress related genes.

1. Introduction

Human health risk assessment of environmental contaminants is a complex process that is mostly conducted on individual compounds. However, the general population is exposed to chemical mixtures acting through multiple pathways. Despite considerable efforts over the past years (Bopp et al. 2019), the improvement of experimental methods for evaluating adverse effects from combined exposure to hazardous chemicals remains a research challenge. The concept of New Approach Methodologies (NAMs) has boosted the development of alternative methods to animal testing, aligning with societal concerns and pursuing the implementation of current regulatory requirements (Ball et al. 2022). Of particular interest is the adoption of cell-based models, which stand out as highly effective for mechanistically based toxicological studies. Moreover, these models have demonstrated a significant potential to analyze the complexities of environmental mixtures (Luo et al.

2022).

In a previous work (Soto-Bielicka et al. 2023), we demonstrated the adequacy of fish cell lines to reliably assess the toxic effects caused by combined exposure to the well-known flame-retardant tetrabromobisphenol A (TBBPA) and polystyrene nanoparticles (PSNPs), two representatives of emerging contaminants in the aquatic environment. Our results revealed subtle changes in cell viability as well as the generation of oxidative DNA damage after co-exposure to subcytotoxic concentrations of the tested pollutants. It should be noted that, as summarized in recent reviews, both TBBPA (Miao et al. 2023) and plastic particles (Malafaia and Barcel   2023) have been also consistently identified in human biological samples, raising further concerns about potential health risks for the general population. Limited data exist concerning toxic effects caused by combined exposure to TBBPA and other environmental pollutants in human cells, particularly micro and nano-sized plastic materials, except for a study in Caco-2 cells using polyethylene

* Correspondence to: Department of Biology, Faculty of Sciences, Universidad Aut  noma de Madrid, 2 Darwin Street, Madrid 28049, Spain.

E-mail addresses: patricia.sotob@estudiante.uam.es (P. Soto-Bielicka), ana.peropadre@uam.es (A. Peropadre), soledad.sanz@uam.es (S. Sanz-Alf  rez), mariajose.hazen@uam.es (M.J. Hazen), paloma.fernandez@uam.es (P. Fern  ndez Freire).

¹ Orcid 0000-0003-4696-852X

² Orcid 0000-0002-0787-9391.

³ Orcid 0000-0003-0858-4963.

⁴ Orcid 0000-0002-6729-5347

⁵ Orcid 0000-0003-1357-8955.

microplastics (Huang et al. 2021). In this cell line, it has been shown that combined exposure to PSNPs and silver-derived substances slightly modulates some adverse cellular effects of silver (Domenech et al. 2021a).

The experimental approach outlined in this study aims to build upon our previous findings conducted with fish cell cultures (Soto-Bielicka et al. 2023), with a specific focus on the effects of TBBPA and PSNPs exposure in human intestinal cells. In order to investigate relevant toxicological endpoints and the underlying cellular mechanisms, we selected the widely used absorptive Caco-2 and the goblet-like HT29-MTX cell lines (Gagnon et al. 2013), as well as their co-culture system, which facilitates the analysis of their interactions (Kuppusamy et al. 2020). Both TBBPA (Hays and Kirman, 2019) and PSNPs (Materić et al. 2022) can be found in natural matrices, so their possible interaction is a subject of interest. Furthermore, TBBPA has the potential to accumulate in humans, especially after repeated exposures (Covaci et al. 2009), and PSNPs might bioaccumulate when ingested by aquatic organisms (Nelms et al. 2018; Zaki and Aris, 2022). Another challenge concerning PSNPs is the difficulty in accurately measuring environmental levels, as there are complexities for their quantification in aquatic media (Koelmans et al. 2015) and human food (EFSA, 2016).

Under these circumstances, to gain insight into their mechanism of toxic action, we followed a conventional approach using a wide concentration range of TBBPA and PSNPs (Zhou et al. 2020), which aligns well with other *in vitro* studies (Honkisz and Wójtowicz, 2015; Jarosiewicz et al. 2019; Wu et al. 2018). Our findings suggest that acute exposure to TBBPA-PSNPs combinations elicit distinct cytotoxic and genotoxic effects on human intestinal cells compared to individual treatments. Noteworthy, the co-culture system yielded the most relevant results, underscoring its applicability for toxicological studies.

2. MATERIALS AND METHODS

2.1. Cell cultures

The human colorectal cancer cell lines Caco-2 (ATCC HTB-37; Virginia, USA) and HT29-MTX (ECACC 15121711; Salisbury, UK) were routinely grown in ventilated 75 cm² flasks (BioLite, Fisher Scientific, Madrid, Spain) in a HERAcell 150i incubator (Thermo Fisher, Karlsruhe, Germany) at 37 °C, with a 5% CO₂ humidified atmosphere and subculture twice a week at 70 – 80% confluence. Complete medium with the following composition was used: high glucose Dulbecco's Modified Eagle's Medium (DMEM) with sodium pyruvate (#SH30243, Cytiva HyClone Laboratories, Utah, USA), 1% penicillin/streptavidin, 1% non-essential aminoacids and 10% fetal bovine serum (FBS), all from Gibco (Life Technologies, New York, USA). Sterile Phosphate Buffer Saline (PBS) and trypsin 2.5%, were obtained from HyClone. Morphological evaluation of cultures was performed with a phase-contrast inverted microscope (Leica DMi1, Leica Microsystems, Wetzlar, Germany).

2.2. Polystyrene nanoparticle characterization.

Carboxylated polystyrene nanoparticles (PSNPs, CML Latex beads) with a 40 nm nominal size were acquired from Thermo Fisher (#11590066) and dispersed in complete medium with or without FBS prior to the analysis. Size distribution by hydrodynamic light scattering (DLS) and zeta potential measures were performed at 25 °C in a Malvern Zetasizer nano ZS (Malvern Instruments Ltd., Worcestershire, UK) kindly provided by Dr. Roberto Rosal (Universidad de Alcalá). Complementary transmission electron microscopy (TEM) studies were conducted as previously reported (Soto-Bielicka et al. 2023) at the "Centro de Biología Molecular Severo Ochoa" facilities on a JEM1400 Flash microscope (Jeol, Tokyo, Japan).

2.3. Cytotoxicity assessment

Cells were seeded on flat transparent 96-well plates at 2×10^5 (Caco-2) or 1.5×10^5 (HT29-MTX) cells/mL for individual cultures. Co-culture systems were established with a 9:1 ratio (Caco-2: HT29-MTX) and a seeding density of 2×10^5 cells/mL, to adequately represent the physiological proportion of goblet cells in the human small intestine (Chen et al. 2010; Karam, 1999). Working solutions of TBBPA (MilliporeSigma, Munich, Germany) were prepared in complete medium from a 0.1 M stock in dimethyl sulfoxide (Serva, Heidelberg, Germany) in a wide range of concentrations (1 – 150 µM, 0.54 – 81.6 µg/mL). A 30 min sonicated stock of 10 mg/mL PSNPs in MilliQ water was used to prepare the final PSNPs working dispersions in complete medium ranging from 0.1 to 200 µg/mL.

Three complementary viability endpoints, Alamar Blue (AB, metabolic activity), carboxyfluorescein diacetate acetoxyethyl ester (CFDA-AM, plasma membrane integrity), and neutral red uptake (NRU, lysosomal integrity) were evaluated on the same multiwell plate following Schirmer et al. (1997). In brief, at treatment termination cells were incubated for 30 min with a combination of AB (5% v/v, Invitrogen, ThermoFisher Scientific) and 4 µM CFDA-AM (Invitrogen) in DMEM without phenol red. Fluorescence was sequentially measured at 530 / 590 nm and 485 / 528 nm excitation/emission for AB and CFDA-AM respectively on a TECAN Infinite 200 PRO M Plex (Tecan Iberica Instrumentación SL, Barcelona, Spain). After discarding the AB-CFDA solution, cells were incubated for 1 h with 40 µg/mL NR, washed, and NR was extracted and fluorescently measured at appropriate wavelengths (530 nm excitation / 645 nm emission) on the same plate reader. The background fluorescence was subtracted from the values obtained before normalization with control untreated cells.

2.4. Evaluation of the oxidative metabolism

Reactive oxygen species (ROS) production and the inner mitochondrial membrane potential at selected experimental conditions were quantified using the fluorescence probes 2', 7' - dichlorofluorescein diacetate (H₂DCFDA, Sigma) and tetramethylrhodamine methyl ester (TMRM, Invitrogen) as previously described (Soto-Bielicka et al. 2023).

In addition, the expression of three relevant genes related to the oxidative stress response (GSTP1, glutathione S-transferase pi 1; NRF2, nuclear erythroid factor-like factor 2; and SOD2, superoxide dismutase 2) was determined. After treatments, cells grown on 6-well plates were trypsinized and the total RNA from 2×10^5 cells/mL was extracted using the RNeasy Mini Kit (Quiagen #74106, Venlo, Netherlands) according to provider instructions. RNA quality was determined using a Nanodrop (ThermoFisher Scientific) and PCR on agarose/polyacrylamide gel. Real-time RT-qPCR analysis was performed on the Genomic Unit of the "Parque Científico de Madrid" using 18 S and CycloB as housekeeping genes. The primers used are listed in Table S1.

2.5. DNA damage assessment

The evaluation of genotoxicity and/or DNA damage was performed by two versions of the comet assay: alkaline and combined with formamidopyrimidine DNA glycosylase (FPG) enzymatic treatment, to determine single and double-strand breaks, and the oxidation product 8-oxo-7, 8-dihydroguanine. After treatments, cells grown on 6-well plates were trypsinized and processed following the methodology proposed by Huarte et al. (2021) with minor modifications (Soto-Bielicka et al. 2023). Briefly, cells were embedded in minigels on agarose-coated microscope slides (2 minigels per slide, 3 slides per condition), immersed in lysis buffer, washed in cold PBS, and incubated at 37 °C either with 1 U FPG (New England Biosciences, Massachusetts, USA) in appropriate buffer, only with buffer or maintained in lysis buffer (not incubated). After rinsing in cold PBS and 30 min unwinding, electrophoresis was performed (30 min, 0.73 V / cm). Finally, slides were rinsed in cold PBS

and distilled water, dehydrated and nucleoids stained with GelRed (Biotium, California, USA). An Olympus BX-61 microscope (Tokyo, Japan) equipped with a camera (Olympus DP70) was used to capture 10 – 15 field images that were processed with the free CometScore 2.0 software (TriTek corp., Virginia, USA) to obtain the % of tail DNA of at least 50 nucleoids per minigel.

In addition, the potential activation of DNA damage genes ATM (mutated ataxia telangiectasia), ATR (ataxia telangiectasia-related protein and Rad3), PARP1 (Poly-(ADP Ribose) Polymerase 1) and OGG1 (8-oxoguanine DNA glycosylase 1) was determined by gene-expression analysis using real-time RT-qPCR as previously explained for the oxidative stress genes. The oligonucleotides used are presented in [Table S1](#).

2.6. Statistical analysis

All the graphical representations and appropriate statistical analysis were performed with GraphPad Prism 9.0 (GraphPad Software, San Diego, USA). Unless otherwise stated, at least three independent experiments were done for all the experimental procedures with a variable number of technical replicates, reported on the figure legends. After removing the outliers, normality and homoscedasticity analysis preceded the statistical analysis including ANOVA or Kruskal-Wallis along with multiple comparisons. Individual and combined dose-responses

modeling and calculation of the Benchmark Dose Responses (BMD) were performed using the software package PROAST version 70.3 for R (4.2.0) developed by the Dutch National Institute for Public Health and the Environment. [Supplementary Figures 2 and 3](#) show the different models obtained with PROAST for Caco 2 and the co-culture of Caco 2 / HT29-MTX respectively.

3. RESULTS

3.1. The cytotoxic effect of TBBPA is different in the co-culture system compared to single intestinal human cell lines.

The assessment of cellular viability on Caco-2, HT29-MTX, and their co-culture after 24 h exposure to TBBPA indicates that metabolic activity (AB) is the most sensitive endpoint ([Fig. 1](#)). We found statistically significant differences with control untreated cells for the AB measurements at TBBPA concentrations ≥ 50 (co-culture), ≥ 100 (Caco-2), or ≥ 125 μM (HT29-MTX). Remarkably, no evident cytotoxicity was detected with the co-culture when evaluating the integrity of plasma membranes (CFDA-AM) or lysosomes (NRU). On the other hand, TBBPA presented differences with control cells with concentrations of ≥ 100 μM on Caco-2 cells for those same parameters. The HT29-MTX cell line appears as the less sensitive to TBBPA exposure, with a slight reduction in CFDA-AM at the highest concentration tested and at ≥ 125 μM TBBPA for NRU. Calculation of BDR (benchmark dose response) values ([Table S2](#)) reveals

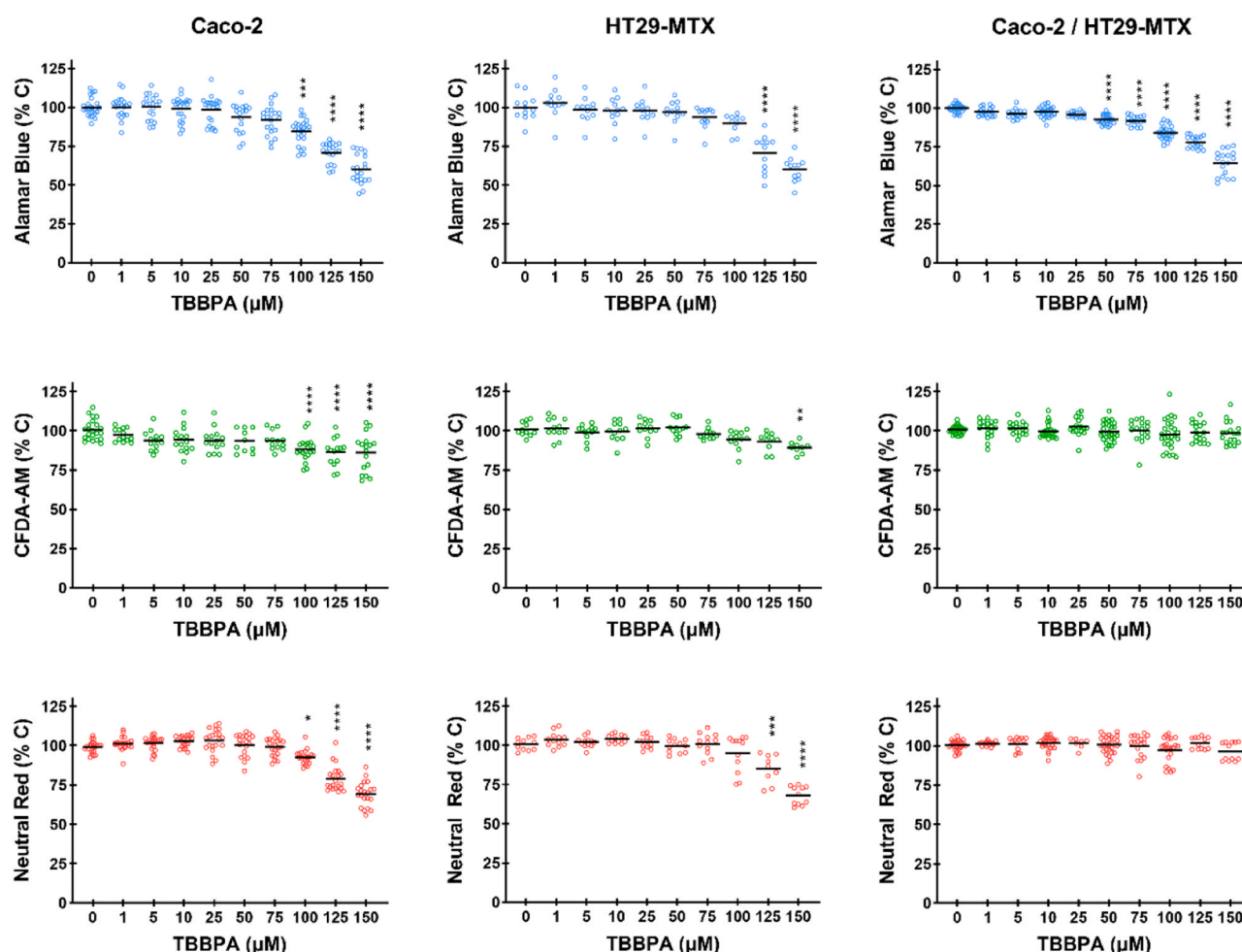


Fig. 1. Cytotoxicity of TBBPA after 24 h exposure in the intestinal cell lines evaluated. Results for metabolic activity (AB), plasma (CFDA-AM), and lysosomal (NRU) membrane integrity are represented by scatter plots showing the individual values and the mean (line). Differences with control cells were considered significant for $p < 0.05$ (*), $p < 0.01$ (**), $p < 0.001$ (***) or $p < 0.0001$ (****) after Kruskal-Wallis + Dunn (AB; CFDA-AM HT29-MTX; NR Caco-2 and co-culture), one-way ANOVA + Dunnett (CFDA-AM Caco-2) or Brown-Forsythe & Welch ANOVA + Dunnett T3 (NR HT29-MTX; CFDA-AM co-culture). $n = 3$ (2 for HT29-MTX); 3–6 technical replicates.

lower and upper limits in agreement with the effect on the metabolic activity of the co-culture, suggesting a differential behavior from the individual cell lines.

3.1. Polystyrene nanoparticles (PSNPs) exert no relevant cytotoxicity on the cellular models employed

The characterization of PSNPs in our exposure media is shown in Table 1 and Fig. 2. Similar behavior was observed for the two concentrations used (1 and 50 µg/mL) in the different exposure media, with a slight increase in Z-average with complete medium at $t = 0$ that returned to values similar to those of freshly prepared dispersions in medium without FBS after a 24 h period (Table 1). TEM images of PSNPs in complete medium (Fig. 2A-D) reveal mainly monodispersed rounded nanoparticles for the lowest concentration and the presence of some aggregates for the 50 µg/mL dispersion, especially after 24 h incubation (Fig. 2E).

Measure conditions: T = 25 °C; dispersant RI 1.330 and viscosity 0.08872 cP; material RI 1.59

Regarding the effects upon cellular function after 24 h exposure (Fig. 3 and Figure S1), PSNPs showed different cytotoxicity for Caco-2 cells alone and their co-culture with HT29-MTX. No evident cellular damage was recorded for Caco-2 cells, despite a dose-independent significant reduction of plasma membrane integrity. On the other hand, the co-culture system showed early signs of reduction in metabolic activity even with low concentrations (0.5 µg/mL). These effects slightly increase at the higher concentrations but could be altogether considered mild.

3.2. The influence of PSNPs upon TBBPA cytotoxicity is evident at lower TBBPA concentrations in the co-culture system

A selection of PSNPs and TBBPA concentrations was used in combination studies to evaluate their potential interactions with cellular functions. TBBPA choices cover three representative concentrations: one where no effect is expected (10 µM), the first that shows differences with control cells in cytotoxicity evaluation (50 µM), and one considered high (100 µM). Regarding PSNPs, as no dose response was observed, the three concentrations selected cover a low (1 µg/mL), an intermediate (10 µg/mL), and a relatively high (50 µg/mL) exposure condition. Fig. 4 shows the results of cytotoxicity assays in the co-culture system after 24 h exposure to TBBPA alone or in combination with PSNPs. Although a

Table 1

DLS measurements of PSNPs in our experimental conditions (n = 3), showing mean ± SD values.

PSNPs	Dispersant	Incubation time (h)	Z-average (d.nm)	Main peak ^a (d.nm)	Polydispersity index (PDI)
10 mg/mL	H ₂ O		50.68 ± 0.14	55.71 ± 19.41	0.165 ± 0.009
1 µg/mL	Medium w/o FBS	0	84.63 ± 2.65	40.2 ± 4.52	0.271 ± 0.019
	Complete medium	0	100.89 ± 0.91	45.77 ± 9.94	0.568 ± 0.010
	Complete medium	24	80.37 ± 0.19	45.2 ± 11.52	0.661 ± 0.002
50 µg/mL	Medium w/o FBS	0	53.41 ± 0.90	60.33 ± 20.06	0.097 ± 0.008
	Complete medium	0	102.00 ± 1.31	127.60 ± 54.45	0.425 ± 0.034
	Complete medium	24	62.82 ± 1.17	94.02 ± 46.65	0.329 ± 0.052

^aRefers to the main peak in size distribution by intensity

clear pattern could not be observed, the individual exposure to 10 µM TBBPA showed statistically significant differences when combined with 10 or 50 µg/mL PSNPs for CFDA-AM, and only with 50 µg/mL PSNPs for AB. The combinations with 50 µM TBBPA reported identical results for CFDA-AM, while no differences were observed for AB. Furthermore, the highest TBBPA concentration was not modified by the addition of any PSNP concentration, and the lysosomal integrity was not altered in any of the evaluated conditions.

The analysis of benchmark doses with the same combination studies for Caco-2 / HT29-MTX co-cultures and Caco-2 (Table 2, Figures S2 and S3) supports the predominant role of TBBPA in the combined exposures, as well as the higher sensitivity of the CFDA-AM endpoint in both experimental systems. Overall, the behavior of the co-culture system was different from Caco-2 cells (Figure S4), being slightly more susceptible to the combined treatments.

3.3. Oxidative metabolism is affected by combined TBBPA and PSNPs treatments.

We evaluated the oxidative status of the co-culture system after selected treatments with TBBPA and PSNPs alone or in combination, using direct measures for ROS and inner mitochondrial membrane potential ($\Delta\Psi_m$), along with changes in the expression of selected genes of the oxidative stress response.

The direct quantification of ROS (Fig. 5A) revealed only a slight significant increase in the co-cultures exposed for 24 h to 100 µM TBBPA either alone or with 50 µg/mL PSNPs. For this endpoint, the presence of PSNPs had apparently no influence on the effects induced by TBBPA alone. In contrast, different statistically significant changes in the $\Delta\Psi_m$ could be observed (Fig. 5B). Dual modifications of this fluorescence measure were recorded, with the highest single TBBPA concentration being the only one to significantly reduce $\Delta\Psi_m$. On the other hand, individual 50 µg/mL PSNPs exposure significantly increased $\Delta\Psi_m$. Interestingly, both combination treatments showed a relevant rise when compared with control untreated co-cultures and also with their respective individual TBBPA concentrations.

We also measured the expression levels of three genes related to the oxidative stress response. The overall behavior of GSTP1, NRF2, and SOD2 follows a common pattern. No changes in expression levels were detected in individual exposures to TBBPA and PSNPs, but exposures to 10 µM TBBPA + 50 µg/mL PSNPs revealed an increase for the three selected genes, with statistically significant differences only for NRF2 and SOD2. Treatments with the highest concentration of TBBPA seemed to reduce the expression of GSTP1 and SOD2, and the addition of PSNPs switched that tendency either to near control values or to overexpression, but no statistical significance was observed.

3.4. Genotoxicity and DNA damage response are triggered after exposures to TBBPA and PSNP combinations

Direct measures of DNA damage with the classical alkaline comet assay of Caco-2 / HT29-MTX co-cultures in selected 24 h treatments revealed a significant effect only after joint exposures of TBBPA and PSNPs (Fig. 6A). Furthermore, the combination exposures also presented higher and statistically significant differences compared with the individual exposure to TBBPA. However, when the FPG-modified comet assay version was used to assess potential oxidative DNA damage (Fig. 6B), relevant differences with control cells were only observed for individual 50 µg/mL PSNPs and 100 µM TBBPA treatments. Interestingly, no differences were observed between those individual exposures and their derived combinations.

The study of the expression changes of the DNA stress response-related genes ATM, ATR, PARP1, and OGG1 showed a common pattern (Fig. 6C). PSNPs 50 µg/mL caused non-significant repression of ATM and ATR, and no changes in PARP1 and OGG1. Likewise, TBBPA alone induced slight repression (ATM, ATR, OGG1) or overexpression

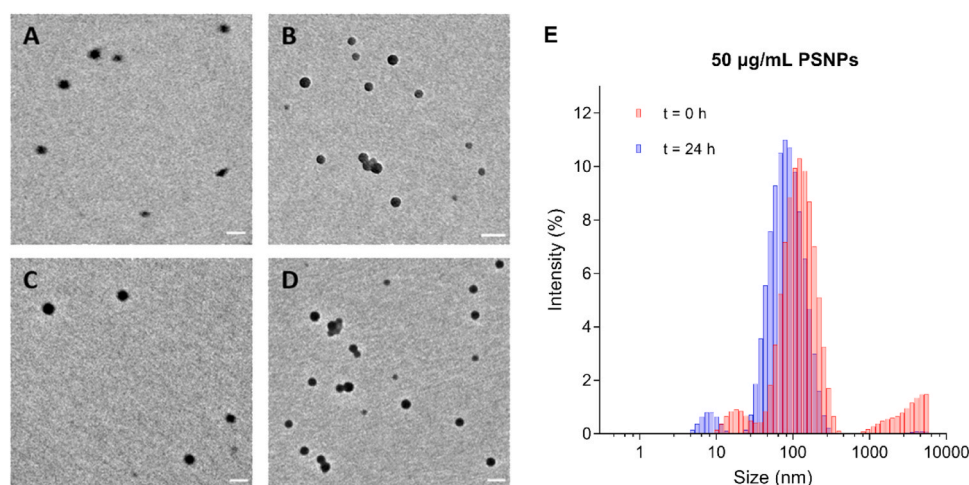


Fig. 2. Characterization of PSNPs in complete medium. Representative images of (A) 1 µg/mL freshly prepared; (B) 50 µg/mL freshly prepared; (C) 1 µg/mL after 24 h incubation at 37 °C; (D) 50 µg/mL after 24 h incubation at 37 °C. (E) Size distribution of 50 µg/mL PSNPs freshly prepared and after 24 h incubation at 37 °C. Scale = 100 nm.

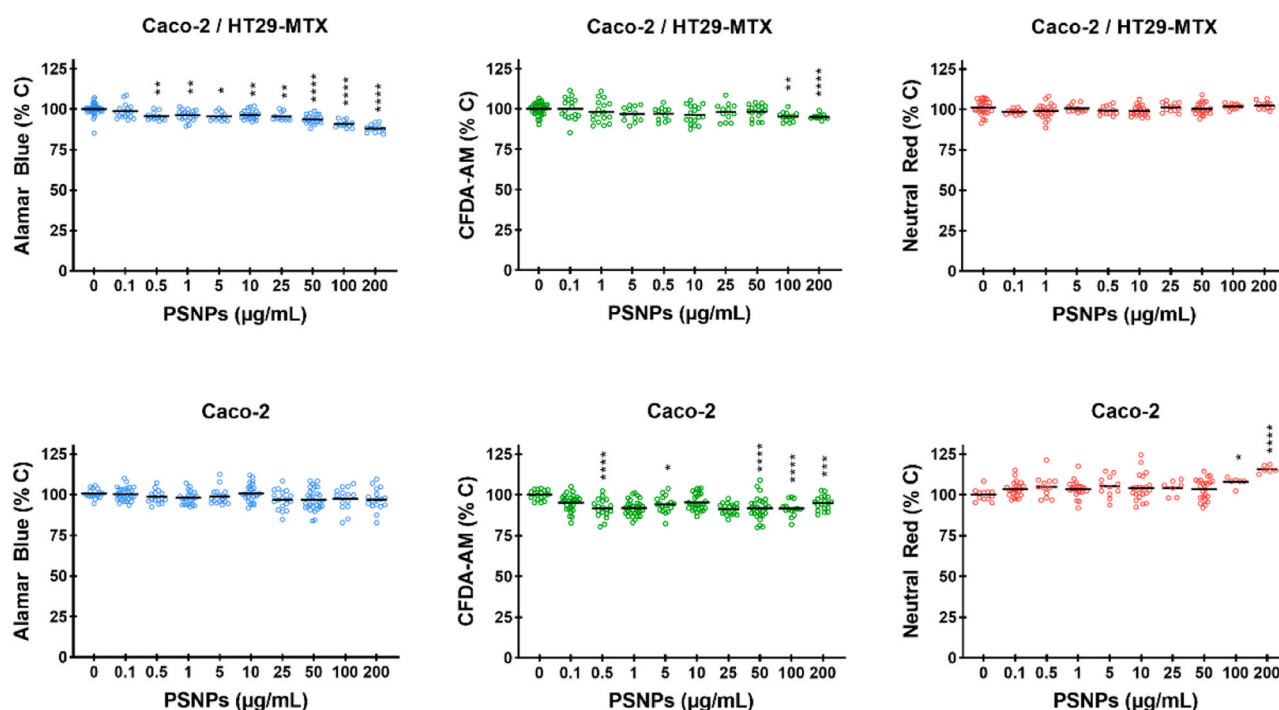


Fig. 3. Cytotoxicity of PSNPs on Caco-2 and Caco-2/HT29-MTX co-culture after 24 h exposure. Results for metabolic activity (AB), plasma (CFDA-AM), and lysosomal (NRU) membrane integrity are represented by scatter plots showing the individual values and the mean (line). Differences with control cells were considered significant for $p < 0.05$ (*), $p < 0.01$ (**), $p < 0.001$ (***) or $p < 0.0001$ (****) after one-way ANOVA + Dunnett (AB, CFDA-AM & NRU Caco-2 and NRU co-culture), Kruskal-Wallis + Dunn (AB co-culture) or Brown-Forsythe & Welch ANOVA + Dunnett T3 (CFDA-AM co-culture). $n = 2$; 5–6 technical replicates.

(PARP1), not significant in any condition. Regarding combined exposures, 10 µM TBBPA + 50 µg/mL PSNPs was the only condition that produced statistically significant modifications when compared with individual 10 µM TBBPA for all the genes studied. The only exception was a no significant PARP1 overexpression, similar to that of TBBPA alone. The combination of 100 µM TBBPA + 50 µg/mL PSNPs presented an identical behavior as TBBPA individually.

4. DISCUSSION

A variety of non-animal methodologies is available for toxicity testing, with current efforts focused on selecting the most suitable

models for extrapolating the data obtained in experimental conditions to human risk assessment. Our study aimed to understand the potential risks of TBBPA and PSNPs mixtures to human health, from a mechanistically based cellular perspective. Because ingestion is the main route of exposure for both compounds in the general population (Domenech et al. 2021a; Okeke et al. 2022), we selected human intestinal cells as the most appropriate *in vitro* model to determine relevant biological endpoints.

First, we studied the cytotoxic effects induced after a single exposure to TBBPA and PSNPs in different cellular settings. Caco-2 cells exhibited more significant changes than HT29-MTX cells, most likely because of their undifferentiated state and low or no cytochrome P450 activity

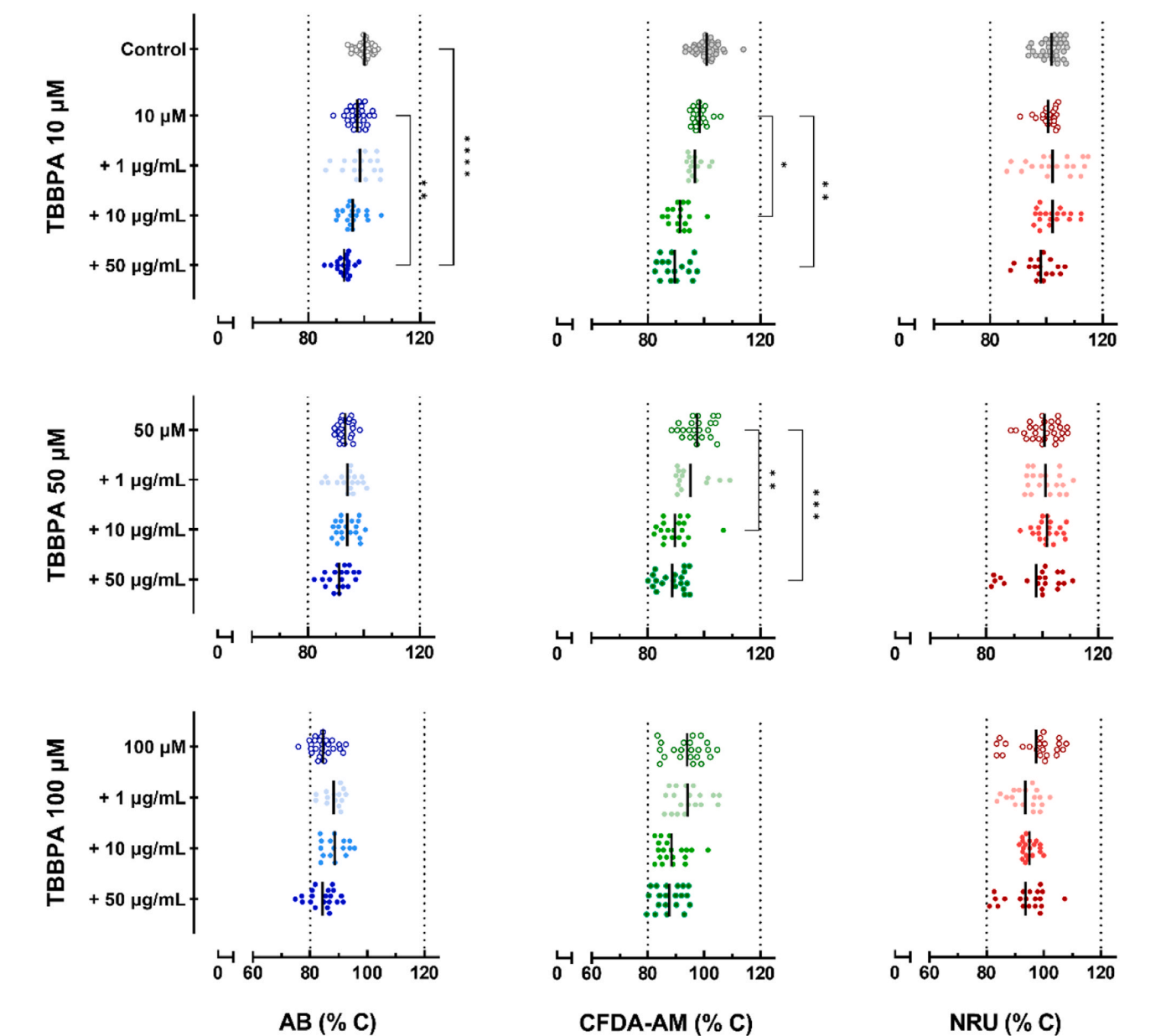


Fig. 4. Cytotoxicity of the combined exposure to TBBPA and PSNPs on Caco-2/HT29-MTX co-cultures during 24 h. Scatter plot representations show the individual values and the mean (line) of the mixtures (TBBPA + 1, 10, and 50 $\mu\text{g/mL}$ PSNPs) for AB (left), CFDA-AM (center), and NRU (right). Asterisks (*) indicate statistically significant differences after Brown-Forsythe & Welch ANOVA + Dunnett T3 tests. $p < 0.05$ (*), $p < 0.01$ (**), $p < 0.001$ (***) or $p < 0.0001$ (****). $n = 3$; 5 technical replicates.

Table 2
Values of benchmark doses (BMD_{lower} and BMD_{upper}) obtained for the combined cytotoxicity assays to assess the BDR.

		Caco-2		Caco-2/HT29-MTX	
AB	TBBPA (CED)	BMD _{low}	BMD _{up}	BMD _{low}	BMD _{up}
	PSNPs (RPF)	37.3	54.7	31.1	46.6
CFDA-AM	TBBPA (CED)	-	-	0.53	0.84
	PSNPs (RPF)	0.529	12.5	16.8	59.6
NRU	TBBPA (CED)	0.01	0.26	1.53	6.95
	PSNPs (RPF)	65.2	86.2	88.7	128
		-	-	0.2	1.14

CED: Critic effective dose
RPF: Relative potency factor

(Ozawa et al., 2015; Küblbeck et al., 2016). Interestingly, the co-culture system (Caco-2/HT29-MTX) was more resistant to TBBPA treatments than the individual cell lines for all the evaluated parameters. HT29-MTX cells are specialized in mucus secretion, which is capable of trapping and altering the toxic effects of chemical compounds present in the exposure medium (Gillois et al., 2018). In the case of TBBPA, mucus could have a protective role as only high concentrations exerted detrimental effects. Remarkably, the results obtained in the co-culture showed metabolic activity alterations at concentrations $\geq 50 \mu\text{M}$ TBBPA, which may be explained by the modulatory effects of HT29-MTX on Caco-2 cells, as previously reported for these cell lines in co-culture (Berger et al. 2017).

The individual exposure to PSNPs was conducted after their characterization in culture media. The proteins present in the serum seem to stabilize PSNPs, preventing the formation of aggregates possibly through the formation of a biocorona, as has already been reported for

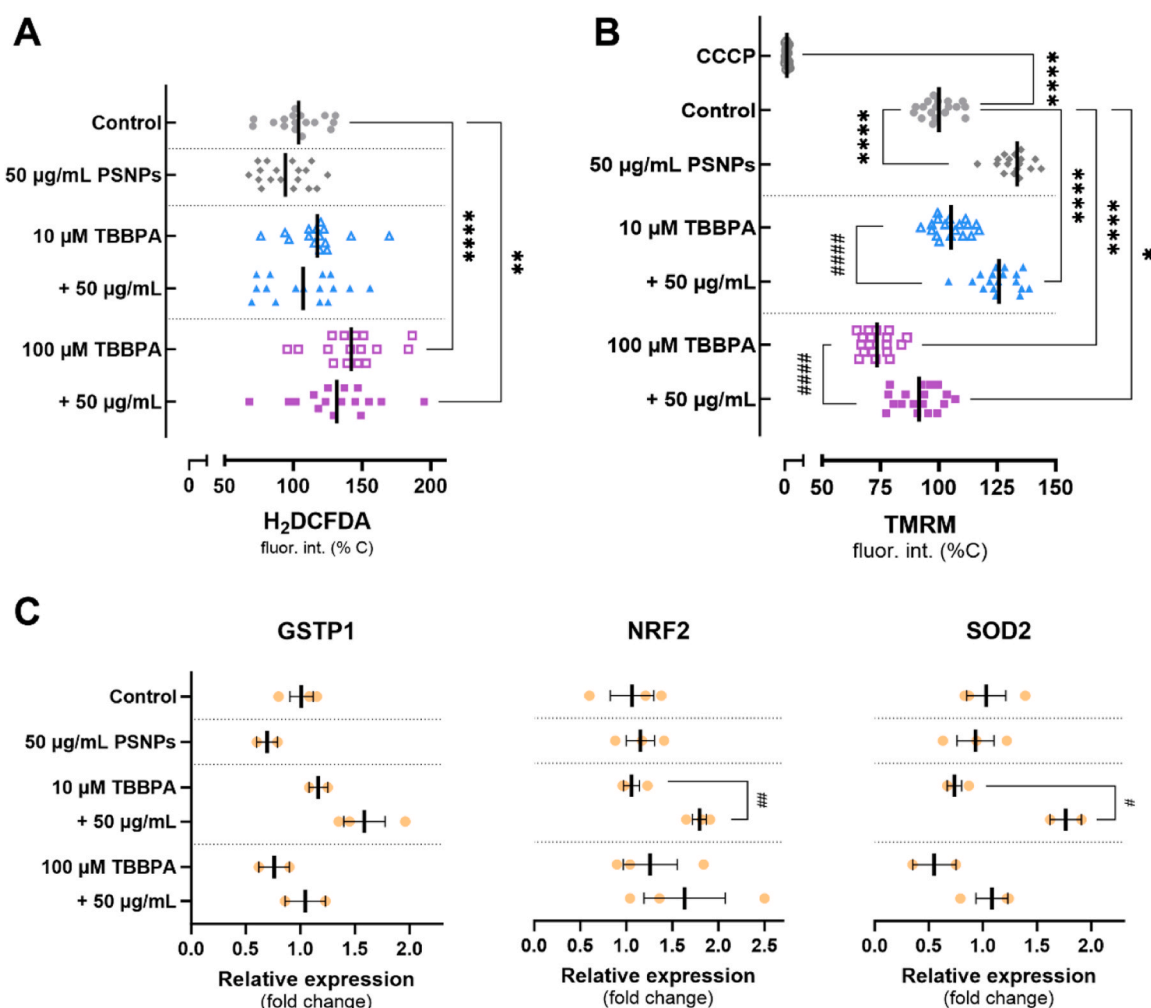


Fig. 5. Oxidative stress response after exposure to selected TBBPA-PSNPs combinations on the Caco-2/HT29-MTX co-culture for 24 h. Scatter plot representations show individual values and the mean \pm SD of (A) ROS production using the fluorescent probe H₂DCFDA, (B) mitochondrial membrane potential measured with TMRM, and (C) relative expression (fold change) of oxidative stress-related genes (GSTP1, NRF2, and SOD2) using the 2- $\Delta\Delta$ CT method. Asterisks (*) indicate statistically significant differences with the control cells, and hashtags (#) with individual TBBPA exposures after One-way ANOVA + Dunnett (A), Brown-Forsythe & Welch ANOVA + Dunnett T3 (B), and One-way ANOVA + Šidák (C) tests. n = 3; 6 (A, B) or 2 (C) technical replicates.

these (Almeida et al. 2019), and other nanoparticles (Lammel and Sturve, 2018). The Z potential value obtained is congruent with the carboxylated nature of these PSNPs and comparable to that determined in other culture media (Hesler et al. 2019). Mild cytotoxic effects were observed on our cellular systems, even after single PSNPs treatments at high concentrations (200 µg/mL), although different susceptibilities for the co-culture could be detected. Similar to that observed after TBBPA exposure, metabolic activity was significantly reduced even with low PSNPs concentrations, while no effects were detected on the plasma membrane and lysosomal integrity. These results reinforce the idea that HT29-MTX cells could render Caco-2 cells more susceptible to chemical exposure at a metabolic level (Berger et al. 2017), although the low cytotoxicity detected is coherent with observations made in other types of intestinal cells, both differentiated (Hesler et al. 2019; Domenech et al. 2021b) and undifferentiated (Wu et al. 2019; Cortés et al. 2020).

The second set of experiments was conducted to determine the potential influence of PSNPs on TBBPA cytotoxicity with selected concentrations (TBBPA 10, 50, and 100 µM; 1, 10, and 50 µg/mL PSNPs) based on our previous results. We found that the influence of PSNPs in the TBBPA-PSNPs mixtures is very small or has no effect at all in the Caco-2 cell line. In the co-culture, we observed a slight reduction of AB with 10 µM TBBPA + 50 µg/mL compared to TBBPA alone, while a more relevant effect on the integrity of the plasma membrane was identified

with CFDA-AM. A similar influence of PSNPs could be detected in combinations with 50 µM TBBPA, reflecting a fairly consistent profile. Nevertheless, when using the highest concentration of TBBPA (100 µM), the results were uninfluenced by PSNPs, presumably due to the prevalence of the flame-retardant cytotoxicity. These findings indicate that the impact of the TBBPA-PSNPs combinations on cell viability does not follow a general pattern among different cell lines and exposure systems, as we have previously described for fish cells (Soto-Bielicka et al. 2023). It is tempting to suggest that our results could be partially explained by the “trojan effect” or vehiculation processes (Wang et al. 2013), in which TBBPA adsorbs on PSNPs. This adsorption probably depends on hydrophobic and electrostatic interactions, as explained for other types of microplastics (Li et al. 2021), although their precise interaction has not been yet studied in detail. Nevertheless, the negative charge of PSNPs plays an important role in the formation of the biocorona (Monopoli et al. 2012; Liu et al., 2022), and thus in the adsorption of TBBPA on these nanoparticles.

The next step in our study includes a more mechanistic approach, focusing on the oxidative stress, and the DNA damage response only in the co-culture setting. Regarding ROS production, both TBBPA and nanoparticles have been reported to generate oxidative stress (Wu et al. 2018; He et al. 2020; Włuka et al. 2020), although we have only observed significant differences with control cells using the highest

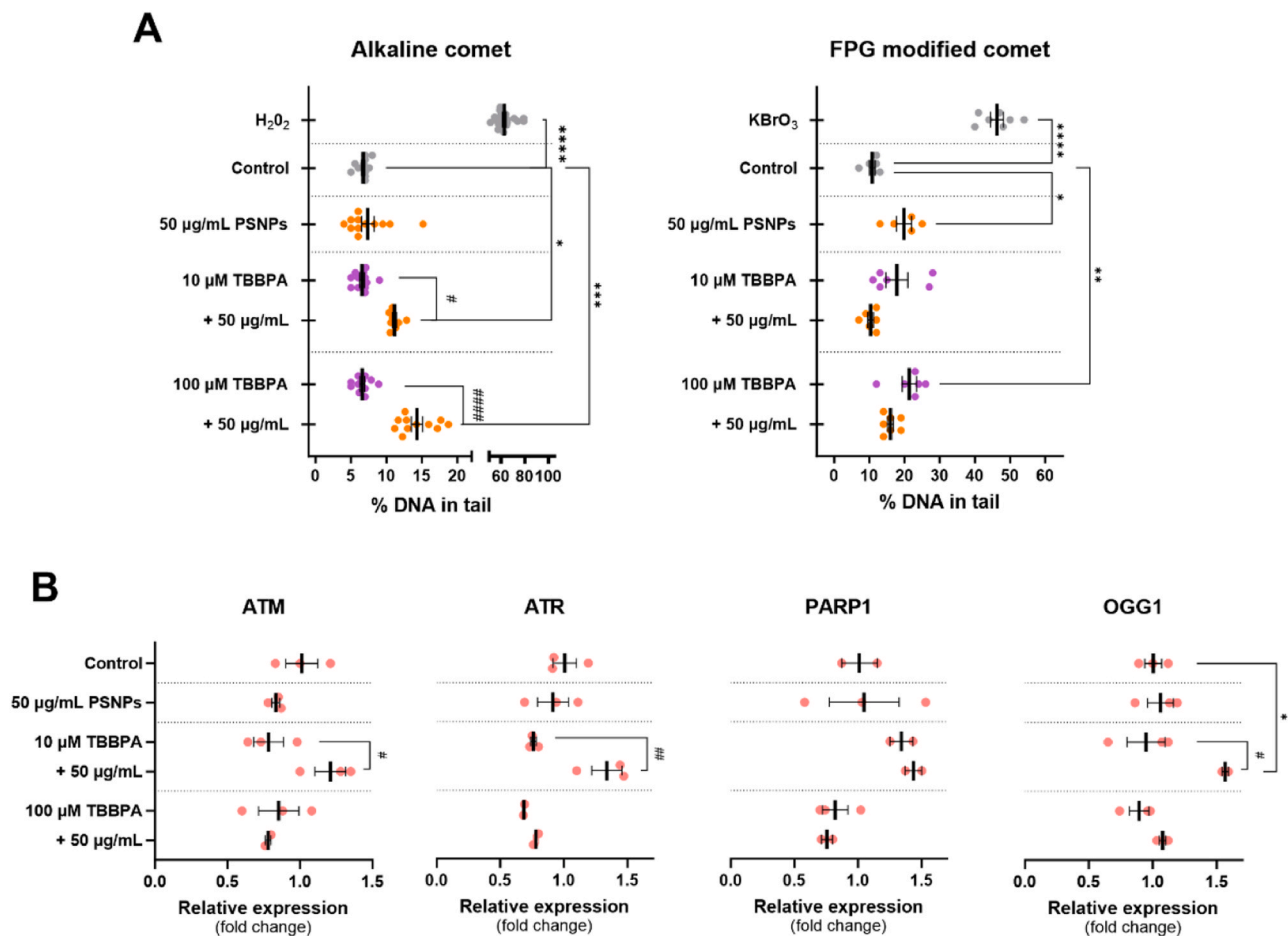


Fig. 6. DNA damage response after exposure to selected TBBPA-PSNPs combinations on the Caco-2/HT29-MTX co-culture for 24 h. Scatter plot representations show individual values and the mean \pm SD of (A) alkaline or FPG-modified Comet assay, and (B) relative expression (fold change) of DNA stress response-related genes (ATM, ATR, PARP1, and OGG1) using the $2^{-\Delta\Delta CT}$ method. Asterisks (*) indicate statistically significant differences with the control cells, and hashtags (#) with individual TBBPA exposures after Kruskal – Wallis + Dunn (A) and One-way ANOVA + Šidák (B) tests. $n = 3$; 3 (A) or 2 (B) technical replicates.

concentration of TBBPA, both individually and in combination with the PSNPs. No differences between individual and combined exposure were found, indicating once again that TBBPA is the main responsible for the observed response. Other authors have reported synergistic effects when evaluating oxidative stress of TBBPA-PSNPs combinations in *Caenorhabditis elegans* (Zhao et al. 2023), suggesting that the cellular system has a major influence on the generation of oxidative stress.

Considering that mitochondria are one of the main endogenous sources of ROS, we evaluated their status with a fluorescence measure of the inner mitochondrial membrane potential ($\Delta\Psi$) in the same experimental conditions used to measure ROS levels. The individual treatments with TBBPA only showed a relevant reduction in $\Delta\Psi$ values after exposure to 100 μ M. Interestingly, we could observe a peculiar increase in $\Delta\Psi$ in all the treatments containing PSNPs, leading to statistically significant differences with both control co-cultures and individual exposures to TBBPA. A similar condition has been reported for low doses of amine-modified PSNPs in primary murine macrophages (Deville et al. 2020) and for PSNPs in Caco-2 cells (Cortés et al. 2020), attributing it to the regulation of the mitochondrial permeability transition pore. However, Perini et al. (2022) suggested that the interaction of PSNPs with phospholipid membranes can cause their hyperpolarization either by stimulating the exit of internal cations through selective pores when they adhere to the membrane surface, or by the internalization of the negatively charged PSNPs. Thus, our results suggest that in combined treatments, the hyperpolarization of the inner mitochondrial membrane caused by PSNPs could alleviate to some extent the effects of TBBPA.

We also determined the expression levels of three genes involved in antioxidant mechanisms in the same conditions of ROS and $\Delta\Psi$ studies. Our results indicate that the combination of 10 μ M TBBPA + 50 μ g/mL PSNPs presents significant differences with 10 μ M TBBPA for NRF2 and SOD2 genes. SOD2 is responsible for converting the superoxide anion into H_2O_2 , which is transformed into H_2O by CAT (catalase; Suski et al. 2018). H_2O_2 can act as a molecular mediator for the NRF2 signaling pathway, enabling it to translocate into the nucleus and induce the expression of many genes (Zhang and Hannink, 2003), including GSTP1. The latter is part of a key system for redox homeostasis, encoding the phase II detoxification enzyme glutathione S-transferase, which conjugates endogenous and exogenous components to the glutathione molecule to reduce oxidative stress (Wang et al. 2015). Although not significant, we could also observe increased gene expression for GSTP1, suggesting that the combination of 10 μ M TBBPA + 50 μ g/mL PSNPs induces the expression of oxidative stress-related genes in our experimental conditions. To our knowledge, there are no studies regarding changes in the expression of these genes after TBBPA-PSNPs joint exposures using mammalian cells. However, the NRF2 gene and some of its targets have been evaluated in human hepatocytes treated with TBBPA (Zhang et al. 2019), showing similar results to ours. In addition, our data coincide with those previously obtained for the GSTP1 and SOD2 genes in human intestinal cells treated with carboxylated PSNPs, where no significant effects were observed, even at high concentrations (Cortés et al. 2020; Domenech et al. 2021b).

We also analyzed the genotoxic potential of the TBBPA-PSNPs

combinations in the co-culture system using the alkaline Comet assay to evaluate the presence of single (SSBs) and double-strand breaks (DSBs), as well as the FPG version to detect the ROS-susceptible modified base 8-oxo-7,8-dihydroguanine. Additionally, real-time qRT-PCR was used to quantify changes in the expression levels of the representative DNA damage response genes ATM, ATR, PARP1, and OGG1. We detected relevant differences with the alkaline comet assay between the two TBBPA-PSNPs combinations evaluated (10 and 100 μ M TBBPA + 50 μ g/mL PSNPs) and both, their respective individual exposures to TBBPA and control co-cultures. These results indicate that the different TBBPA-PSNPs combinations can produce DNA breaks, which has also been observed by Domenech et al. (2021a) for combinations of PSNPs with silver nanoparticles or silver nitrate. However, the FPG comet assay only showed differences with control conditions for 100 μ M TBBPA, either in single or combination exposure. Thereby, high concentrations of TBBPA can cause oxidative DNA damage, according to our previous results detecting ROS in those same experimental conditions. However, our work using the RTgill-W1 fish cell line (Soto-Bielicka et al. 2023) provided somewhat opposite results, which might be explained by the different exposure conditions (concentrations used, composition of exposure media) and cellular sensitivities. Nevertheless, it seems that in the human intestinal co-culture system, TBBPA induces oxidative stress, which could lead to DNA damage. In good agreement, TBBPA has the potential to act as a free radical itself (Szychowski and Wójtowicz, 2016). As for the PSNPs, also considering our results in the $\Delta\Psi$ studies, they could play a protecting role against oxidative stress damage in the different combinations of TBBPA-PSNPs.

Regarding the analysis of DNA damage-related genes, the combination of 10 μ M TBBPA + 50 μ g/mL PSNPs exerts a significant increase in the expression of all the evaluated genes, except for PARP1, when compared to the individual TBBPA exposure. It is especially noteworthy that for OGG1 there is a significant difference from control co-cultures, indicating that, indeed, certain oxidative DNA damage is being produced and not detected in any other condition. Since PARP1 inhibits the activity of OGG1 (Noren Hooten et al. 2011), this would explain why there are no differences in the evaluation of PARP1 while there is an increase in the expression of OGG1.

In conclusion, despite the slight enhancement of the effects of TBBPA by PSNPs, we propose that the adverse effects observed on human intestinal cells are primarily driven by TBBPA and strongly influenced by the specific experimental cellular context. Particularly interesting findings emerged from the use of the more physiologically relevant intestinal co-culture system, underscoring its significance in toxicological studies. It is imperative to develop and provide standardized cellular-based non-animal systems to better evaluate the potential risks associated with chemical exposure, also incorporating different pathological conditions.

Declarations

na

Ethical approval

Not applicable.

Funding

This work was funded by the Spanish Ministry of Science, Innovation and Universities / Spanish State Research Agency / RTI2018-096046-B-C22 and PID2022-141894OB-C22. PSB has benefited from a contract from the Office of Education and Research of the Community of Madrid and the European Social Fund (PEJ-2019-AI/SAL-12775).

CRedit authorship contribution statement

Patricia Soto-Bielicka: Investigation, Formal analysis, Data curation. **Ana Peropadre:** Writing – original draft, Supervision, Methodology, Investigation, Formal analysis, Conceptualization. **Soledad Sanz-Alferez:** Investigation, Formal analysis. **M^a José Hazen:** Writing – review & editing, Conceptualization. **Paloma Fernández Freire:** Writing – review & editing, Writing – original draft, Visualization, Supervision, Project administration, Funding acquisition, Formal analysis, Data curation, Conceptualization.

Declaration of Competing Interest

The authors have no relevant financial or non-financial interests to disclose.

Data Availability

Data will be made available on request.

Acknowledgments

This work was funded by the Spanish Ministry of Science, Innovation and Universities / Spanish State Research Agency / RTI2018-096046-B-C22, PID2022-141894OB-C22. PSB has benefited from a contract from the Office of Education and Research of the Community of Madrid and the European Social Fund (PEJ-2019-AI/SAL-12775).

Appendix A. Supporting information

Supplementary data associated with this article can be found in the online version at doi:10.1016/j.tox.2024.153769.

References

- Almeida, M., Martins, M.A., Soares, A.M.V., Cuesta, A., Oliveira, M., 2019. Polystyrene nanoplastics alter the cytotoxicity of human pharmaceuticals on marine fish cell lines. *Environ. Toxicol. Pharm.* 69, 57–65. <https://doi.org/10.1016/j.etap.2019.03.019>.
- Ball, N., Bars, R., Botham, P.A., Cuciureanu, A., Cronin, M.T.D., Doe, J.E., Dudzina, T., Gant, T.W., Leist, M., van Ravenzwaay, B., 2022. A framework for chemical safety assessment incorporating new approach methodologies within REACH. *Arch. Toxicol.* 96, 743–766. <https://doi.org/10.1007/s00204-021-03215-9/TABLES/7>.
- Berger, E., Nassra, M., Atgié, C., Plaisancié, P., Gélöen, A., 2017. Oleic Acid Uptake Reveals the Rescued Enterocyte Phenotype of Colon Cancer Caco-2 by HT29-MTX Cells in Co-Culture Mode. *Int J. Mol. Sci.* 18, 1573. <https://doi.org/10.3390/IJMS18071573>.
- Bopp, S.K., Kienzler, A., Richarz, A.N., van der Linden, S.C., Paini, A., Parissis, N., Worth, A.P., 2019. Regulatory assessment and risk management of chemical mixtures: challenges and ways forward. *Crit. Rev. Toxicol.* 49, 174–189. <https://doi.org/10.1080/10408444.2019.1579169>.
- Chen, X.M., Elisia, I., Kitts, D.D., 2010. Defining conditions for the co-culture of Caco-2 and HT29-MTX cells using Taguchi design. *J. Pharm. Toxicol. Methods* 61, 334–342. <https://doi.org/10.1016/j.vascn.2010.02.004>.
- Cortés, C., Domenech, J., Salazar, M., Pastor, S., Marcos, R., Hernández, A., 2020. Nanoplastics as a potential environmental health factor: Effects of polystyrene nanoparticles on human intestinal epithelial Caco-2 cells. *Environ. Sci. Nano* 7, 272–285. <https://doi.org/10.1039/c9en00523d>.
- Covaci, A., Voorspoels, S., Abdallah, M.A.E., Geens, T., Harrad, S., Law, R.J., 2009. Analytical and environmental aspects of the flame retardant tetrabromobisphenol-A and its derivatives. *J. Chromatogr. A* 1216, 346–363. <https://doi.org/10.1016/j.chroma.2008.08.035>.
- Deville, S., Honrath, B., Tran, Q.T.D., Fejer, G., Lambrichts, I., Nelissen, I., Dolga, A.M., Salvati, A., 2020. Time-resolved characterization of the mechanisms of toxicity induced by silica and amino-modified polystyrene on alveolar-like macrophages. *Arch. Toxicol.* 94, 173–186. <https://doi.org/10.1007/s00204-019-02604-5/FIGURES/5>.
- Domenech, J., Cortés, C., Vela, L., Marcos, R., Hernández, A., 2021a. Polystyrene Nanoplastics as Carriers of Metals. Interactions of Polystyrene Nanoparticles with Silver Nanoparticles and Silver Nitrate, and Their Effects on Human Intestinal Caco-2 Cells. *Biomolecules* 11, 859. <https://doi.org/10.3390/Biom11060859>.
- Domenech, J., de Britto, M., Velázquez, A., Pastor, S., Hernández, A., Marcos, R., Cortés, C., 2021b. Long-Term Effects of Polystyrene Nanoplastics in Human Intestinal Caco-2 Cells. *Biomolecules* 11, 1442. <https://doi.org/10.3390/Biom11101442>.

- EFSA, 2016. Presence of microplastics and nanoplastics in food, with particular focus on seafood—EFSA Panel on Contaminants in the Food Chain (CONTAM). *EFSA J.* 14 e04501.
- Gagnon, M., Zihler Berner, A., Chervet, N., Chassard, C., Lacroix, 2013. Comparison of the Caco-2, HT-29, and the mucus-secreting HT29-MTX intestinal cell models to investigate Salmonella adhesion and invasion. *J. Microbiol. Methods*, 94:274–9. <https://www.doi.org/10.1016/j.mimet.2013.06.027>.
- Hays, S.M., Kirman, C.R., 2019. Biomonitoring Equivalents (BEs) for tetrabromobisphenol A. *Regul. Toxicol. Pharm.* 102, 108–114. <https://doi.org/10.1016/j.yrtph.2018.12.014>.
- He, Y., Li, J., Chen, J., Miao, X., Li, G., He, Q., Xu, H., Li, H., Wei, Y., 2020. Cytotoxic effects of polystyrene nanoplastics with different surface functionalization on human HepG2 cells. *Sci. Total Environ.* 723, 138180 <https://doi.org/10.1016/j.scitotenv.2020.138180>.
- Hesler, M., Aengenheister, L., Ellinger, B., Drexler, R., Straskraba, S., Jost, C., Wagner, S., Meier, F., von Briesen, H., Büchel, C., Wick, P., Buerki-Thurnherr, T., Kohl, Y., 2019. Multi-endpoint toxicological assessment of polystyrene nano- and microparticles in different biological models in vitro. *Toxicol. Vitro* 61, 104610 <https://doi.org/10.1016/j.tiv.2019.104610>.
- Honkisz, E., Wójcicki, A.K., 2015. The role of PPAR γ in TBBPA-mediated endocrine disrupting effects in human choriocarcinoma JEG-3 cells. *Mol. Cell Biochem* 409, 81–91. <https://doi.org/10.1007/s11010-015-2514-z>.
- Huang, W., Yin, H., Yang, Y., Jin, L., Lu, G., Dang, Z., 2021. Influence of the co-exposure of microplastics and tetrabromobisphenol A on human gut: Simulation in vitro with human cell Caco-2 and gut microbiota. *Sci. Total Environ.* 778, 146264 <https://doi.org/10.1016/j.scitotenv.2021.146264>.
- Huarte, E., Cid, C., Azqueta, A., de Peña, M.-P., 2021. DNA damage and DNA protection from digested raw and griddled green pepper (poly)phenols in human colorectal adenocarcinoma cells (HT-29). *Eur. J. Nutr.* 60, 677–689. <https://doi.org/10.1007/s00394-020-02269-2>.
- Jarosiewicz, M., Krokosz, A., Marczak, A., Bukowska, B., 2019. Changes in the activities of antioxidant enzymes and reduced glutathione level in human erythrocytes exposed to selected brominated flame retardants. *Chemosphere* 227, 93–99. <https://doi.org/10.1016/j.chemosphere.2019.04.008>.
- Karam, S.M., 1999. Lineage commitment and maturation of epithelial cells in the gut. *Front Biosci.* 4, D286–D298. <https://doi.org/10.2741/karam>.
- Koelmans, A.A., Besseling, E., Shim, W.J., 2015. Nanoplastics in the aquatic environment. Critical review. *Mar. Anthropol. Litter* 325–340. https://doi.org/10.1007/978-3-319-16510-3_12.
- Kuppusamy P., Kim D., Soundharajan I., Hwang I., Choi K.C. Adipose and Muscle Cell Co-Culture System: A Novel In Vitro Tool to Mimic the In Vivo Cellular Environment. *Biology* 2021, Vol 10, Page 6. 2020;10:6. <https://doi.org/10.3390/BIOLOGY10010006>.
- Lammel, T., Sturve, J., 2018. Assessment of titanium dioxide nanoparticle toxicity in the rainbow trout (*Oncorhynchus mykiss*) liver and gill cell lines RTL-W1 and RTgill-W1 under particular consideration of nanoparticle stability and interference with fluorometric assays. *Nanoplastics* 11, 1–19. <https://doi.org/10.1016/j.nimpact.2018.01.001>.
- Li, S., Ma, R., Zhu, X., Liu, C., Li, L., Yu, Z., Chen, X., Li, Z., Yang, Y., 2021. Sorption of tetrabromobisphenol A onto microplastics: Behavior, mechanisms, and the effects of sorbent and environmental factors. *Ecotoxicol. Environ. Saf.* 210, 111842 <https://doi.org/10.1016/j.ecoenv.2020.111842>.
- Liu, S., Junaid, M., Liao, H., Liu, X., Wu, Y., Wang, J., 2022. Eco-corona formation and associated ecotoxicological impacts of nanoplastics in the environment. *Sci Total Environ* 836, 155703. <https://doi.org/10.1016/j.scitotenv.2022.155703>.
- Luo, Y.S., Chen, Z., Hsieh, N.H., Lin, T.E., 2022. Chemical and biological assessments of environmental mixtures: A review of current trends, advances, and future perspectives. *J. Hazard Mater.* 432, 128658 <https://doi.org/10.1016/j.jhazmat.2022.128658>.
- Malafaia, G., Barceló, D., 2023. Microplastics in human samples: Recent advances, hot-spots, and analytical challenges. *TrAC Trends Anal. Chem.* 161, 117016 <https://doi.org/10.1016/j.trac.2023.117016>.
- Materić, D., Peacock, M., Dean, J., Futter, M., Maximov, T., Moldan, F., Röckmann, T., Holzinger, R., 2022. Presence of nanoplastics in rural and remote surface waters. *Environ. Res. Lett.* 17, 054036 <https://doi.org/10.1088/1748-9326/AC68F7>.
- Miao, B., Yakubu, S., Zhu, Q., Issaka, E., Zhang, Y., Adams, M., 2023. A review on tetrabromobisphenol a: human biomonitoring, toxicity, detection and treatment in the environment. *Molecules* 28, 2505. <https://doi.org/10.3390/MOLECULES28062505>.
- Monopoli, M.P., Åberg, C., Salvati, A., Dawson, K.A., 2012. Biomolecular coronas provide the biological identity of nanosized materials. *Nat. Nanotechnol.* 7, 779–786. <https://doi.org/10.1038/NNANO.2012.207>.
- Nelms, S.E., Galloway, T.S., Godley, B.J., Jarvis, D.S., Lindeque, P.K., 2018. Investigating microplastic trophic transfer in marine top predators. *Environ. Pollut.* 238, 999–1007. <https://doi.org/10.1016/j.envpol.2018.02.016>.
- Noren Hooten, N., Kompaniez, K., Barnes, J., Lohani, A., Evans, M.K., 2011. Poly(ADP-ribose) polymerase 1 (PARP-1) binds to 8-oxoguanine-DNA glycosylase (OGG1). *J. Biol. Chem.* 286, 44679–44690. <https://doi.org/10.1074/JBC.M111.255869>.
- Okeke, E.S., Qian, X., Che, J., Mao, G., Chen, Y., Xu, H., Ding, Y., Zeng, Z., Wu, X., Feng, W., 2022. Transcriptomic sequencing reveals the potential molecular mechanism by which Tetrabromobisphenol A bis (2-hydroxyethyl ether) exposure exerts developmental neurotoxicity in developing zebrafish (*Danio rerio*). *Comp. Biochem. Physiol. C. Toxicol. Pharm.*, 109467 <https://doi.org/10.1016/j.cbpc.2022.109467>.
- Perini, D.A., Parra-Ortiz, E., Varó, I., Queral-Martín, M., Malmsten, M., Alcaraz, A., 2022. Surface-Functionalized Polystyrene Nanoparticles Alter the Transmembrane Potential via Ion-Selective Pores Maintaining Global Bilayer Integrity. *Langmuir* 38, 14837–14849. <https://doi.org/10.1021/ACS.LANGMUIR.2C02487>.
- Schirmer, K., Chan, A.G.J., Greenberg, B.M., Dixon, D.G., Bols, N.C., 1997. Methodology for demonstrating and measuring the photocytotoxicity of fluoranthene to fish cells in culture. *Toxicol. Vitro* 11, 107–113. [https://doi.org/10.1016/S0887-2333\(97\)00002-7](https://doi.org/10.1016/S0887-2333(97)00002-7).
- Soto-Bielicka, P., Tejeda, I., Peropadre, A., Hazen, M.J., Fernández Freire, P., 2023. Detrimental effects of individual versus combined exposure to tetrabromobisphenol A and polystyrene nanoplastics in fish cell lines. *Environ. Toxicol. Pharm.* 98, 104072 <https://doi.org/10.1016/j.etap.2023.104072>.
- Suski, J., Lebieczinska, M., Bonora, M., Pinton, P., Duszynski, J., Wieckowski, M.R., 2018. Relation Between Mitochondrial Membrane Potential and ROS Formation. *Methods Mol. Biol.* 1782, 357–381. https://doi.org/10.1007/978-1-4939-7831-1_22.
- Szychowski, K.A., Wójcicki, A.K., 2016. TBBPA causes neurotoxic and the apoptotic responses in cultured mouse hippocampal neurons in vitro. *Pharmacol. Rep.* 68, 20–26. <https://doi.org/10.1016/j.pharep.2015.06.005>.
- Wang, F., Yu, L., Monopoli, M.P., Sandin, P., Mahon, E., Salvati, A., Dawson, K.A., 2013. The biomolecular corona is retained during nanoparticle uptake and protects the cells from the damage induced by cationic nanoparticles until degraded in the lysosomes. *Nanomedicine* 9, 1159–1168. <https://doi.org/10.1016/J.NANO.2013.04.010>.
- Wang, Q., Chuiikov, S., Taitano, S., Wu, Q., Rastogi, A., Tuck, S.J., Corey, J.M., Lundy, S. K., Mao-Draayer, Y., 2015. Dimethyl fumarate protects neural stem/progenitor cells and neurons from oxidative damage through Nrf2-ERK1/2 MAPK pathway. *Int. J. Mol. Sci.* 16, 13885–13907. <https://doi.org/10.3390/IJMS160613885>.
- Witka, A., Woźniak, A., Woźniak, E., Michałowicz, J., 2020. Tetrabromobisphenol A, terabromobisphenol S and other bromophenolic flame retardants cause cytotoxic effects and induce oxidative stress in human peripheral blood mononuclear cells (in vitro study). *Chemosphere* 261, 127705. <https://doi.org/10.1016/J.CHEMOSPHERE.2020.127705>.
- Wu, B., Wu, X., Liu, S., Wang, Z., Chen, L., 2019. Size-dependent effects of polystyrene microplastics on cytotoxicity and efflux pump inhibition in human Caco-2 cells. *Chemosphere* 221, 333–341. <https://doi.org/10.1016/j.chemosphere.2019.01.056>.
- Wu, S., Wu, M., Qi, M., Zhong, L., Qiu, L., 2018. Effects of novel brominated flame retardant TBBPA on human airway epithelial cell (A549) in vitro and proteome profiling. *Environ. Toxicol.* 33, 1245–1253. <https://doi.org/10.1002/TOX.22632>.
- Zaki, M.R.M., Aris, A.Z., 2022. An overview of the effects of nanoplastics on marine organisms. *Sci. Total Environ.* 831, 154757 <https://doi.org/10.1016/J.SCITOTENV.2022.154757>.
- Zhang, D.D., Hannink, M., 2003. Distinct cysteine residues in Keap1 are required for Keap1-dependent ubiquitination of Nrf2 and for stabilization of Nrf2 by chemopreventive agents and oxidative stress. *Mol. Cell Biol.* 23, 8137–8151. <https://doi.org/10.1128/MCB.23.22.8137-8151.2003>.
- Zhang, Y., Wang, X., Chen, C., An, J., Shang, Y., Li, H., Xia, H., Yu, J., Wang, C., Liu, Y., Guo, S., 2019. Regulation of TBBPA-induced oxidative stress on mitochondrial apoptosis in L02 cells through the Nrf2 signaling pathway. *Chemosphere* 226, 463–471. <https://doi.org/10.1016/J.CHEMOSPHERE.2019.03.167>.
- Zhao, K., Zhang, Y., Liu, M., Huang, Y., Wang, S., An, J., Wang, Y., Shang, Y., 2023. The joint effects of nanoplastics and TBBPA on neurodevelopmental toxicity in *Caenorhabditis elegans*. *Toxicol. Res. (Camb.)* 12, 76–85. <https://doi.org/10.1093/TOXRES/TFAC086>.
- Zhou, H., Yin, N., Faiola, F., 2020. Tetrabromobisphenol A (TBBPA): A controversial environmental pollutant. *J. Environ. Sci. (China)* 97, 54–66. <https://doi.org/10.1016/J.JES.2020.04.039>.